Journal of Natural Gas Science and Engineering 23 (2015) 118–126

Contents lists available at ScienceDirect

Journal of Natural Gas Science and Engineering

journal homepage: www.elsevier.com/locate/jngse

Thermal effect on wellbore stability during drilling operation with long horizontal section

Mengbo Li [a, *], Gonghui Liu [a, b], Jun Li [a]

[a] China University of Petroleum, College of Petroleum Engineering, Beijing 102249, China
[b] Beijing Information Science & Technology University, Beijing 100192, China

ARTICLE INFO

Article history:
Received 3 November 2014
Received in revised form
18 January 2015
Accepted 20 January 2015
Available online

Keywords:
Horizontal well drilling
Long horizontal section
Integrated circulation temperature model
Thermal stress
Critical mud weight window
Uncertainty analysis

ABSTRACT

In this study, a three-dimensional wellbore stability model is presented that takes into account thermal stresses combined with an integrated circulation temperature model for horizontal well drilling, the bottom hole temperature simulation were then validated using field measurements, and compared with results for vertical wells. A subsequent analysis of temperature sensitivity revealed that the heat source term, the length of horizontal section and mud specific heat were the main reasons cause the bottom hole temperature for horizontal wells rises above the static formation temperature. Results from the wellbore stability model show that the temperature variation magnitude in horizontal well is smaller than that in vertical wells, however, the effect of thermal stress on critical mud weight window in horizontal is more sensitive. The wellbore at toe of horizontal section is more stable than that at heel of horizontal section when the bottom hole temperature exceeds the static formation temperature. This research can provide a theoretical reference for enhancing overall operational efficiency and safety for horizontal well drilling.

1. Introduction

In oil and gas resource development and exploitation, horizontal wells have been widely used to enhance production by increasing the amount of wellbore that has contact with the target reservoir. Unfortunately, due to high temperature environments that accompany such drilling, severe problems can be encountered such as the instabilities caused by drilling fluids and in-situ stresses.

Many scholars have studied the heat transfer of geothermal systems during drilling operations, using both analytical and numerical methods to estimate the circulating fluid temperature. Analytical methods are generally used for modeling simple drilling systems, for example, with regular wellbore geometry and single temperature gradients (Holmes and Swift, 1970; Ramey, 1962; Edwardson et al., 1962; Tragesser et al., 1967; Kabir and Hasan, 1996). For more complex systems, however, simple analytical methods are unable to accurately model the thermal behavior. Numerical methods are required for studying more complex systems, and to provide a powerful predictive tool that can efficiently solve the governing finite difference equations for unsteady-state heat transfer in both wellbore and formation (Raymond, 1969; Wooley, 1980; Marshall and Bentsen, 1982).

All mentioned above was suit for vertical wells, and some scholars (Perkins and Gonzalez, 1981; Tang and Luo, 1998) presented model predictions of the effect on the near wellbore stresses of different temperature for vertical wells.

More recently, as horizontal well have been widely used, Yoshioka et al. (2007) and Li and Zhu (2010) developed thermal models to predict downhole temperature, pressure and flow rate profiles for horizontal wells, but these models only consider the heat transfer in horizontal section and the reservoir. Kumar et al. (2012a, 2012b) developed a simple analytical model to analyze heat generated from borehole friction and to predict downhole temperatures for extended-reach well drilling operations. Their model applies only to steady-state conditions and therefore does not accurately model the heat transfer processes. Iyoho et al. (2009) discussed the influencing factors on wellbore temperature of horizontal wells with long horizontal or near horizontal sections for mud system design purposes, no theoretical details were revealed. Gonzalez et al. (2004) found that the fracture gradient can be influenced by wellbore temperature through leak-off test. Yu et al. (2001) and Nguyen et al. (2010) modeling the thermal effects on wellbore stability, separately. However, only limited studies

* Corresponding author.
E-mail address: limengbocupb@126.com (M. Li).

http://dx.doi.org/10.1016/j.jngse.2015.01.027
1875-5100/

presently exist that use numerical methods to study the thermal effect on wellbore stability combining with thermal behavior of horizontal well drilling systems, especially with long horizontal section.

The temperature variation in horizontal wells is much different from vertical wells (Trichel and Fabian, 2011), which cause a different thermal effect on wellbore stability along the long horizontal section, thus, we can't study either the temperature model or thermal effect on wellbore stability independently.

Given the above, the objective of our present research was to develop a combined model that would serve to: (i) numerically simulate the heat transfer processes during high temperature drilling operations in horizontal wells, and (ii) determine the thermal effect on wellbore stability under the true downhole drilling environment with long horizontal wells, based on temperature distribution derived from the simulations.

In this study, an integrated circulation temperature model of horizontal well drilling was established to investigate the heat transfer characteristics of horizontal wells. Thermal stress near wellbore of horizontal well were analyzed combining with the true downhole drilling environment, the thermal effects on the "critical mud weight window" was discussed, providing a theoretical reference for better understanding the thermal behavior and thermal effect on wellbore stability in horizontal well drilling operations.

2. Wellbore temperature of horizontal well and influencing factors

2.1. Mathematical model development

A schematic diagram of the horizontal drilling operation is shown in Fig. 1. The whole drilling system has five distinct regions: (1) drilling fluid flow downward through the drill pipe; (2) drill pipe wall region; (3) drilling fluid flow upward through the annular; (4) formation region, and (5) drill bit region. According to the well trajectory, each region can be divided into three parts: vertical section, curved section, and horizontal section (excluding region (5) above).

To develop the energy equations for describing thermal behavior of the entire wellbore profile and surrounding formation, the following assumptions are made:

(1) Only heat conduction in horizontal direction is considered, as the majority of formations drilled are layered rock.
(2) Physical properties of formations, i.e., density, specific heat and thermal conductivity rate are constant; heat conduction only is applied in modeling the formations.
(3) Fluid properties are independent of temperature, and wellbore drilling fluids are incompressible and in steady-state flow during each time step.
(4) Heat transfer within the drilling fluid occurs by axial convection. Conduction is neglected except when the circulation process is terminated.
(5) Horizontal well drilling has a rotational motion drilling, without any buckling.

In applying these equations to model the thermal behavior of the entire drilling system, five different sets of governing differential equations must be defined, one for each of the five regions identified earlier, along with boundary conditions at each interface as determined by flow continuity or other conditions.

2.1.1. The wellbore region

The wellbore region can be divided into three sub-regions which are fluidic region in drill pipe, drill pipe wall region and fluidic region in annular. The energy conservation equations in each sub-region in cylindrical coordinates can be written as the following forms, separately:

$$(\rho C_P)_{flui}\left(\frac{\partial T_{flui,p}}{\partial t}+v_{flui,p}\frac{\partial T_{flui,p}}{\partial z}\right)=\lambda_{flui}\frac{\partial^2 T_{flui,p}}{\partial r^2}+\frac{\lambda_{flui}}{r}\frac{\partial T_{flui,p}}{\partial r}+S_p \tag{1}$$

$$(\rho C_P)_{ste}\frac{\partial T_{pipe}}{\partial t}=\lambda_{ste}\frac{\partial^2 T_{pipe}}{\partial z^2}+\lambda_{ste}\frac{\partial^2 T_{pipe}}{\partial r^2}+\frac{\lambda_{ste}}{r}\frac{\partial T_{pipe}}{\partial r} \tag{2}$$

$$\left(\rho C^P\right)_{mix}\left(\frac{\partial T_{flui,a}}{\partial t}+v_{flui,a}\frac{\partial T_{flui,a}}{\partial z}\right)=\lambda_{mix}\frac{\partial^2 T_{flui,a}}{\partial r^2}+\frac{\lambda_{mix}}{r}\frac{\partial T_{flui,a}}{\partial r}+S_a \tag{3}$$

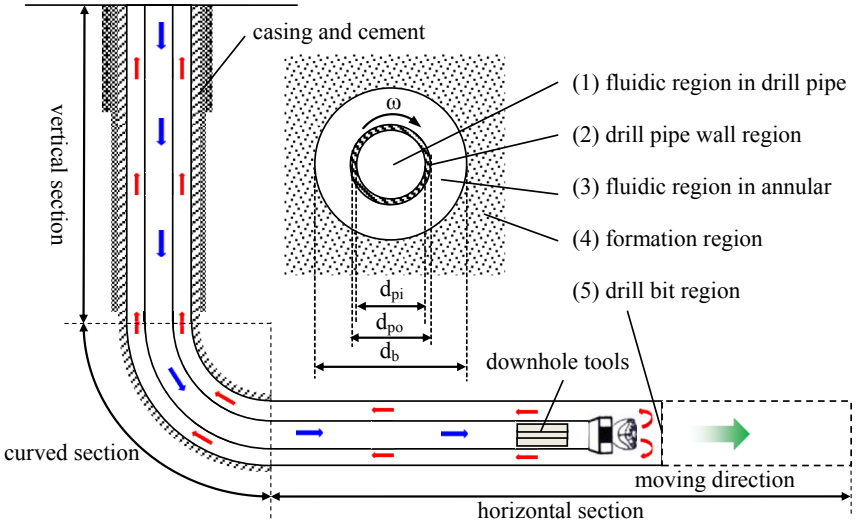

Fig. 1. Illustrative sketch of fluid circulation in horizontal well drilling systems.

2.1.2. Formation region

The formation encountered in well drilling operations is porous medium. Formation porosity must therefore be considered in this region. The formation thermal capacity can be written as (Qiu et al., 2004):

$$(\rho C_P)_{form} = (\rho C_P)_{rock}(1-\Phi) + (\rho C_P)_{poro}\Phi \tag{4}$$

$$\lambda_{form} = \lambda_{poro}^{\Phi} + \lambda_{rock}^{(1-\Phi)} \tag{5}$$

The energy balance equation for the formation regions in vertical and curved section of the wellbore can be written as:

$$(\rho C_P)_{form}\frac{\partial T_{form}}{\partial t} = \lambda_{form}\frac{\partial^2 T_{form}}{\partial r^2} + \frac{\lambda_{form}}{r}\frac{\partial T_{form}}{\partial r} \tag{6}$$

In horizontal drilling section, the axis of the wellbore is parallel with the horizontal direction. Heat conduction both in the axis and radial directions must therefore be considered. Furui et al. (2003) investigated a reservoir inflow model for a horizontal well and approximated the pressure and temperature profile in the reservoir as a composite of 1D radial flow near the well, and a 1D linear flow further away from the well as shown in Fig. 2 below. They estimated that the distance from the wellbore where linear streamlines became radial as H/2, where H is as shown in the Figure.

When there is no fluid flow in the formation (the region of linear streamlines), only heat conduction is considered, the energy balance equation then reduces to:

$$(\rho C_P)_{form}\frac{\partial T_{form}}{\partial t} = \begin{cases} \lambda_{form}\dfrac{\partial^2 T_{form}}{\partial r^2} + \dfrac{\lambda_{form}}{r}\dfrac{\partial T_{form}}{\partial r} + \lambda_{form}\dfrac{\partial^2 T_{form}}{\partial z^2}, & r \le H/2 \\ \lambda_{form}\dfrac{\partial^2 T_{form}}{\partial r^2} + \lambda_{form}\dfrac{\partial^2 T_{form}}{\partial z^2}, & r > H/2 \end{cases} \tag{7}$$

2.2. Model validation

A deep horizontal well (vertical depth 6180 m) in Tarim oilfield, with a long horizontal section (678 m) was selected with actual drilling circulation schedule. This well utilized an 88.9 mm diameter drill pipe set in a 152.4 mm diameter hole, with a very high bottom hole static temperature in the horizontal section of about 150 °C. Oil-based drilling fluid was used for best borehole stability. Rate of penetration varied from 0.71 to 3.76 m/h, with an average rate of 1.6 m/h. The physical properties of materials in drilling circulation system are shown in Table 1.

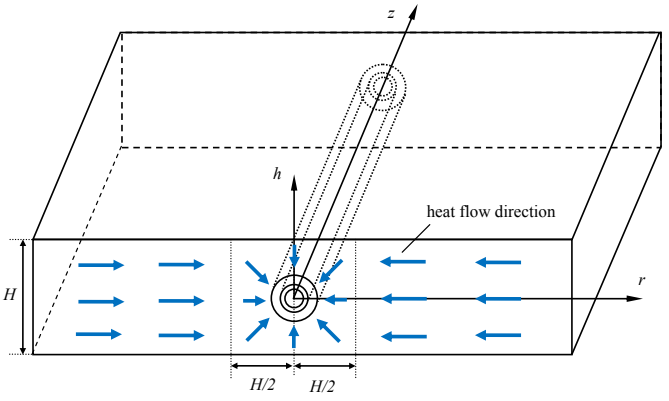

Fig. 2. Schematics of heat transfer between wellbore and formation in horizontal section.

MWD (measurement while drilling) was used to detect downhole annular temperature in both wells. The measured temperature was stored in the downhole tools. The device was able to continuously record the downhole temperature in the annulus during circulation.

Fig. 3 plots the predicted and measured temperatures at different depths during drilling operations. Time-zero was set to coincide with the time that the moving interface was at the landing point (the beginning of the horizontal section). The static temperature profile was used as the starting temperature at the commencement of the simulation. This was not optimal, but after 8 h of simulation, results were seen to be not significantly dependent on the initial conditions any longer. The calculated temperatures were close to measured values, and the bottom hole temperature gradually increased with the measured depth increase, as the drill bit continued to break more rock.

2.3. Influencing factors on wellbore temperature of horizontal well

For vertical wells, the change of wellbore temperature was mainly due to the heat transfer between the formation and wellbore fluid. Because of geothermal gradients, formation temperature varies greatly in the vertical direction. Compared with the heat change caused by geothermal gradients, minor thermal effects such as the heat caused by viscous dissipation in the drilling fluid can be ignored. However, for horizontal wells, the temperature gradient rarely changes in the horizontal section. When sufficient heat transfer occurs between the long horizontal section of the wellbore and the formation, any thermal effect will have a considerable impact on the changes in wellbore temperature.

Fig. 4 shows the calculated heat flux distributions attributable to forced convection, hydraulic energy and mechanical energy hear sources, for various unit control volumes at different sections of the wellbore in horizontal well drilling. The heat transfer and energy source distribution ratios are calculated at the midpoints of the

Table 1
Physical properties of materials in drilling circulation system.

	Density [kg/m^3]	Specific heat [J/(kg °C)]	Thermal conductivity [W/(m °C)]
Rock	2640	837	2.25
Drilling pipe	7800	400	43.75
Cement	1900	2000	1.0
Drilling fluid	1080	1647 (oil based mud)	1.02

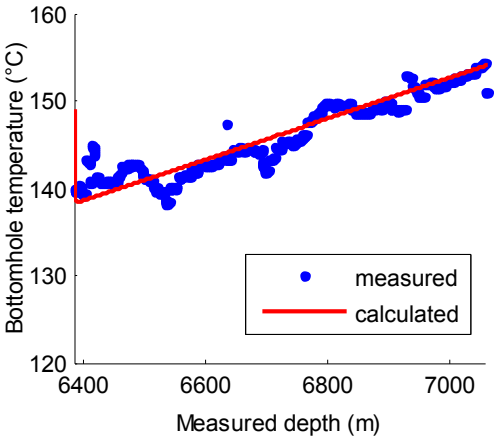

Fig. 3. Trend match of bottom hole temperature measurements with model predictions.

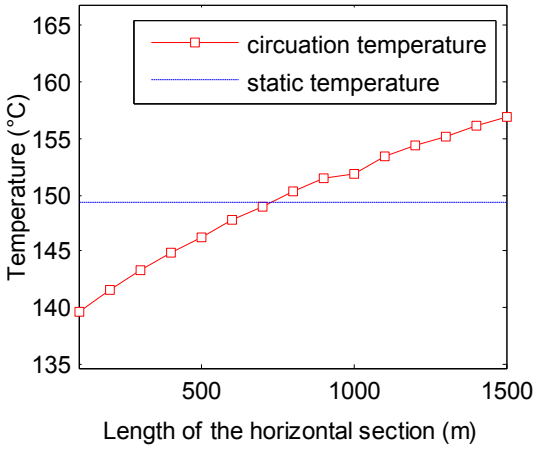

Fig. 5. Effect of horizontal section length on the annular temperature profile.

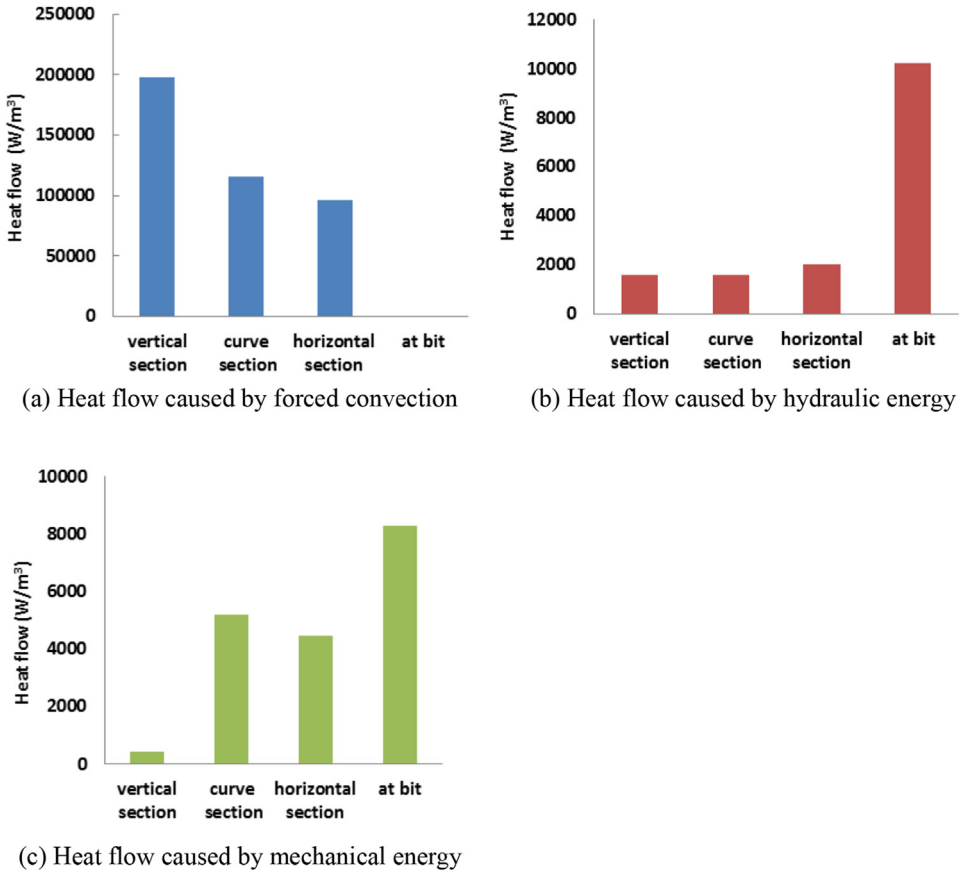

Fig. 4. Comparison of control volume heat flux in different sections of the wellbore.

respective unit control volumes for the vertical section, curved section, horizontal section, and the drill bit section. From Fig. 4, it is apparent that as the depth increases, the transferred heat caused by forced convection in unit control volumes decreases, mainly because the horizontal section is in full contact with the formation, which leads to small changes of fluid temperature in the axial direction. However, the heat generated by hydraulic energy and mechanical energy gradually increases with depth, and displays a significant increase near the drill bit. The heat transfer between the formation and the horizontal section of the wellbore, and mechanical and heat sources themselves are the main reasons for the different (i.e., higher) bottom hole circulating temperatures in horizontal wells versus vertical wells.

The horizontal well geometry and materials physical properties were used as a basis for a sensitivity analysis. The major difference between horizontal wells and vertical wells in temperature profile is that the horizontal section of the wellbore has a sufficient heat transfer with the formations, where the bottom hole static temperature is at its maximum and the temperature gradient rarely changes. The length of the horizontal section reflects the size of the

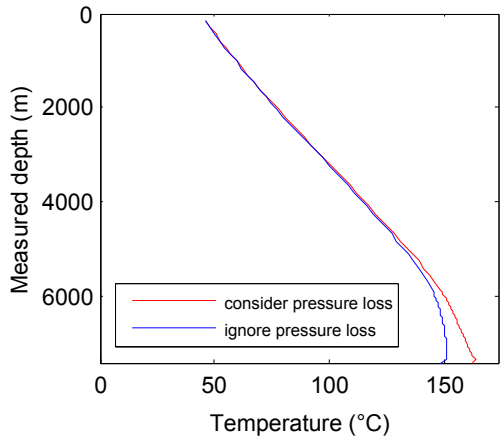

Fig. 6. Effect of BHA pressure drop on the annular temperature profile.

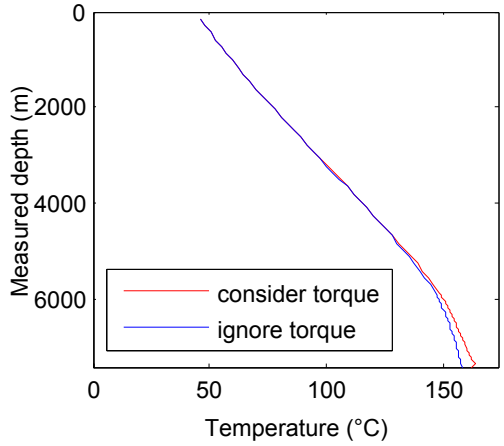

Fig. 7. Effect of torque on the annular temperature profile.

contact surface between the drilling fluid and the formation, as shown in Fig. 5. The bottom hole circulating temperature increases with length of the horizontal section. When this length reaches 700 m or more, the bottom hole circulating temperature exceeds the static formation temperature.

Fig. 6 shows the effect of pressure drop distribution on the wellbore circulation temperature profile. The wellbore circulation temperature profiles of the horizontal section are affected mostly by the pressure drop, which causes an 8 °C increase compared with the bottom hole circulation temperature, without considering the frictional pressure drop in BHA. Fig. 7 shows the effect of the heat source component generated by torque on the annular temperature profile. There is a 3 °C decrease in bottom hole calculation temperature when without considering heat source term of torque.

Fluid systems with different specific heats generally exhibit marked differences in their respective thermal behavior. Fig. 8 demonstrates the effect of different mud systems on borehole circulation temperature profile. The specific heat capacity of water-based mud is about twice that for oil-based mud, resulting in the small temperature gradient of water-based mud in the annular temperature profile. Compared with oil-based mud, the annular temperature profile of water-based mud has a 20 °C decrease in its bottom temperature, and a 7 °C increase in outlet temperature.

Reducing mud pump rate, on the one hand, will reduce convective heat transfer coefficient between the drilling fluid and formation, which in turn results in increased bottom hole

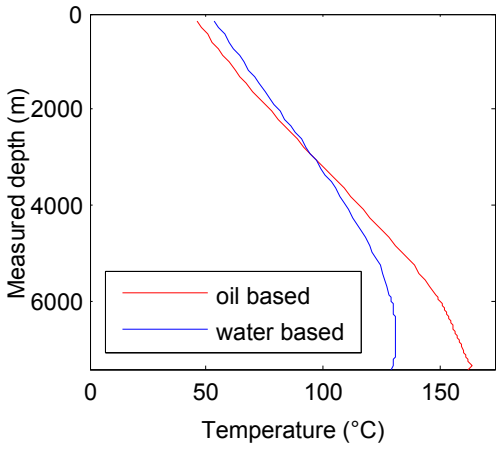

Fig. 8. Effect of mud type (oil-based versus water-based) on annular temperature profile.

circulating temperature. On the other hand, it reduces the pressure loss heat source term generated by the downhole tool, decreasing the bottom hole circulation temperature. Consequently, there is no obvious law between pump rate and bottom hole temperature, and the relationship should be determined according to the specific situation.

3. Thermal stress near wellbore of horizontal well

3.1. Stress induced by formation temperature changes in horizontal well

When the temperature near the wellbore is changed, the thermal stress occurs in the formation. It is well known that the thermal stress occurs only when the heating expansion or cooling shrinkage is restrained. The thermal stress resulting from a temperature change ΔT (T-T_0) for the rock which is fully constrained in one direction is:

$$\sigma_T = E\alpha_T \Delta T \tag{8}$$

where E is Young's modulus and α_T is linear thermal expansion coefficient of rock. If the ΔT is positive, it will cause a tensile stress, and it has an opposite effect when the ΔT is negative.

The stresses induced by thermal effect near wellbore are given as follows:

$$\begin{aligned}
\sigma_r &= -\frac{E\alpha_T}{1-\upsilon}\frac{1}{r^2}\int_R^r \Delta T r dr \\
\sigma_\theta &= \frac{E\alpha_T}{1-\upsilon}\frac{1}{r^2}\left[\int_R^r \Delta T r dr - r^2\Delta T\right] \\
\tau_{r\theta} &= -\frac{E\alpha_T}{1-\upsilon}\Delta T
\end{aligned} \tag{9}$$

A homogeneous and isotropic formation around the wellbore is assumed with constant formation properties. Based on the thermal elastic mechanics theory (Xu, 1982), the thermal effect is considered by adding the thermal induced stress into the pure elastic model (Fjaer et al., 1992), and the stress components can be expressed in cylindrical coordinate (align with the wellbore axes) as follows:

$$\begin{cases} \sigma_r = \dfrac{R^2}{r^2}p_i + \dfrac{(\sigma_{xx}+\sigma_{yy})}{2}\left(1-\dfrac{R^2}{r^2}\right) + \dfrac{(\sigma_{xx}-\sigma_{yy})}{2}\left(1+\dfrac{3R^4}{r^4}-\dfrac{4R^2}{r^2}\right)\cos 2\theta + \delta\left[\dfrac{\alpha_B(1-2\upsilon)}{2(1-\upsilon)}\left(1-\dfrac{R^2}{r^2}\right)-\phi\right](p_i-P_p) - \dfrac{E\alpha_T}{1-\upsilon}\dfrac{1}{r^2}\int_R^r \Delta T r dr \\ \sigma_\theta = -\dfrac{R^2}{r^2}p_i + \dfrac{(\sigma_{xx}+\sigma_{yy})}{2}\left(1+\dfrac{R^2}{r^2}\right) - \dfrac{(\sigma_{xx}-\sigma_{yy})}{2}\left(1+\dfrac{3R^4}{r^4}\right)\cos 2\theta + \delta\left[\dfrac{\alpha_B(1-2\upsilon)}{2(1-\upsilon)}\left(1+\dfrac{R^2}{r^2}\right)-\phi\right](p_i-P_p) + \dfrac{E\alpha_T}{1-\upsilon}\dfrac{1}{r^2}\left[\int_R^r \Delta T r dr - r^2\Delta T\right] \\ \sigma_z{=}\sigma_{zz} + \upsilon\left[\sigma_{xx}+\sigma_{yy}-2(\sigma_{xx}-\sigma_{yy})\left(\dfrac{R}{r}\right)^2\cos 2\theta\right] + \delta\left[\dfrac{\alpha_B(1-2\upsilon)}{1-\upsilon}-\phi\right](p_i-P_p) - \dfrac{E\alpha_T}{1-\upsilon}\Delta T \end{cases} \tag{10}$$

where, the σ_{xx}, σ_{yy}, σ_{zz} shown above are the three in-situ principal stresses around the wellbore, for horizontal well, they have the following equations:

$$\begin{cases} \sigma_{xx} = \sigma_v \\ \sigma_{yy} = \sigma_H \sin a^2\beta + \sigma_h \cos^2\beta \\ \sigma_{zz} = \sigma_H \cos^2\beta + \sigma_h \sin^2\beta \end{cases} \tag{11}$$

At the borehole surface, the equation (10) can be express as follows:

$$\begin{cases} \sigma_r = p_i - \delta\phi(p_i - P_p) \\ \sigma_\theta = -p_i + (1-2\cos 2\theta)\sigma_{xx} + (1+2\cos 2\theta)\sigma_{yy} + \delta\left[\dfrac{\alpha_B(1-2\upsilon)}{(1-\upsilon)}-\phi\right](p_i-P_p) - \dfrac{E\alpha_T}{1-\upsilon}\Delta T \\ \sigma_z{=}\sigma_{zz} - 2\upsilon(\sigma_{xx}-\sigma_{yy})\cos 2\theta + \delta\left[\dfrac{\alpha_B(1-2\upsilon)}{1-\upsilon}-\phi\right](p_i-P_p) - \dfrac{E\alpha_T}{1-\upsilon}\Delta T \end{cases} \tag{12}$$

3.2. Failure of the wellbore

The stresses around the wellbore are then calculated based on the pore pressure and temperature profiles by using the equations shown above. Critical mud weights are determined using Mohr–Coulomb failure criteria and tensile failure criteria,

The Mohr–Coulomb failure criteria has the following forms:

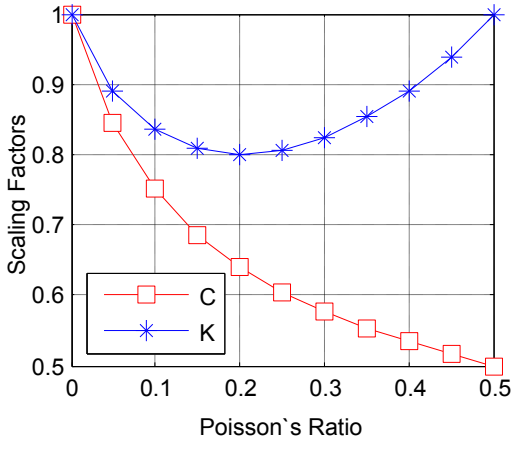

Fig. 9. Scaling factors caused by Poisson's effect (Aadnoy and Belayneh, 2008).

$$(\sigma_{\max} - \alpha P_p) \le 2S_0 \tan\left(\frac{\pi+2\phi}{4}\right) + (\sigma_{\min} - \alpha P_p)\tan^2\left(\frac{\pi+2\phi}{4}\right) \tag{13}$$

As for tensile failure criteria, the effects of Poisson's ratio must be considered. Aadnoy and Belayneh (2008) described the effects of Poisson's ratio on fracturing pressure and thermal stress by using the scaling factor C and K, the temperature effect on the fracturing equation can be expressed as:

$$\sigma_T = KE\alpha_T\Delta T \tag{14}$$

where, $K = (1+\upsilon)^2/(3\upsilon(1-2\upsilon)+(1+\upsilon)^2)$, Fig. 9 shows the magnitude of Poisson's effect.

And the tensile failure criteria can be expressed as:

$$\sigma_{bd} = (\sigma_{\min} - \alpha P_p) + \sigma_t \le 0 \tag{15}$$

The critical mud weight window are computed by use of equations above, the input parameters are given in Table 2 including thermal effects, wellbore information. The examples

Table 2
Input data of formation properties.

Variables	Values
Overburden stress gradient	2.26 Mpa/100 m
Maximum horizontal stress gradient	2.04 MPa/100 m
Minimum horizontal stress gradient	1.88 Mpa/100 m
Pore pressure, equivalent	1.24 g/cm^3
Thermal expansion coefficient	2.36 × 10^{-5} °C^{-1}
Poisson's ratio	0.22
Biot's constant	0.9
Young's modulus	6895 Mpa
Cohesion	6.14 Mpa
Friction angle	30°
Tensile strength	0.69 Mpa

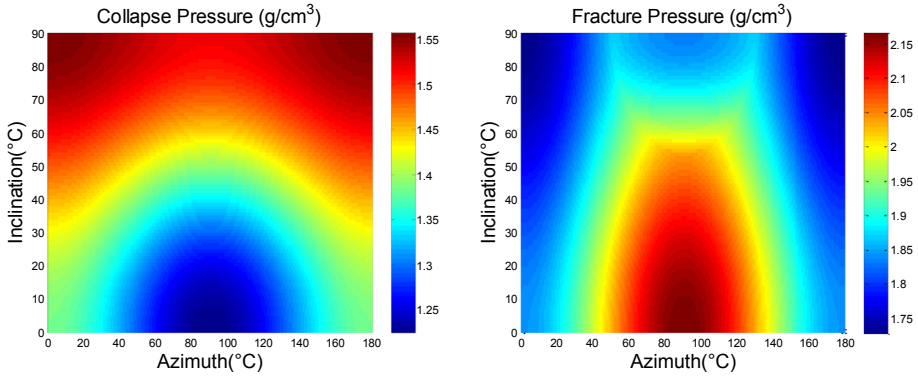

Fig. 10. Effect of inclination angle and azimuth angle on critical mud weights window.

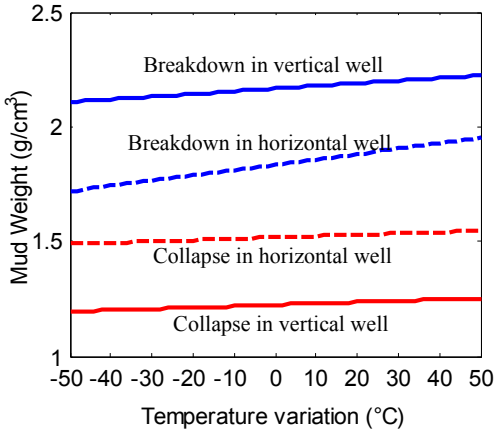

Fig. 11. Effect of temperature on critical mud weight window for vertical and horizontal wellbores.

shown in this paper were based on this input data combining with well geometry and physical properties of materials discussed in Section 2.2.

The minimum and maximum mud weight requirements for both breakdown and collapse as a function of borehole inclinations are plotted, as shown in Fig. 10. As the inclination angle increased, the mud weight for breakdown decreased, and mud weight for collapse increased, which makes the safety mud window of horizontal well narrower than that in vertical well, and the horizontal wellbore is more apt to fracture or collapse.

3.3. Thermal effect on horizontal well

Fig. 11 shows the thermal effect on critical mud weight for vertical and horizontal wells. For vertical well, the breakdown mud weight and collapse mud weight change by 1.16×10^{-3} g/cm^3 and 5.81×10^{-4} g/cm^3 for every 1 °C variation in a vertical well, respectively. A linear relationship of thermal effect on critical mud weight window is also obtained for horizontal wells. However, the thermal effect on horizontal wells is more sensitive than on vertical wells. The breakdown mud weight decreases by 2.32×10^{-3} g/cm^3 for every 1 °C of decreasing for a horizontal well, while the collapse mud weight only has a 5.81×10^{-4} g/cm^3 decreasing, wellbore temperature variation has a greater effect on the formation breakdown pressure than on the formation collapse pressure for both vertical and horizontal wells.

The wellbore is more apt to fracture when the formation temperature is decreased because the cooling effect will cause a tensile stress in circumferential direction which can reduce the hoop stress near wellbore. Increasing the formation temperature increases both the breakdown and collapse mud weights, however presents a smaller effect on collapse mud weight.

Combining with the true drilling condition, critical mud weights of horizontal well along the horizontal section with different mud system are shown in Fig. 12. For oil-based mud, the temperature at the toe of horizontal section is rise above the static formation temperature, and causes a larger critical mud weight window, while opposite situation occurs at the heel of horizontal section.

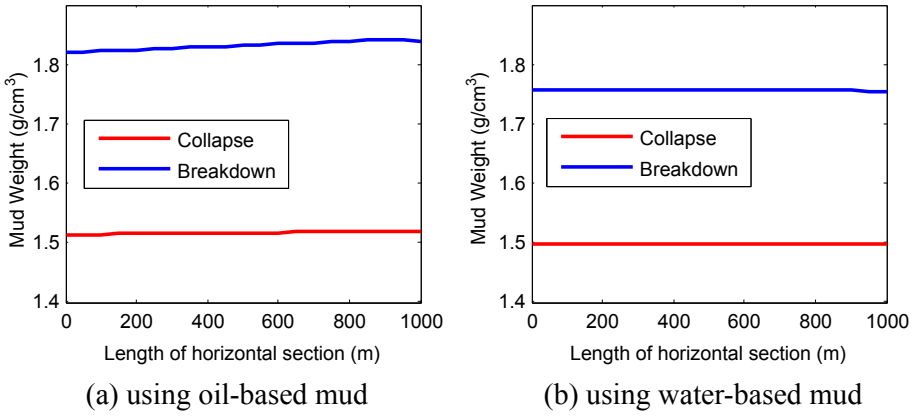

Fig. 12. Critical mud weights window of horizontal well along the horizontal section with different mud system.

Table 3
Sensitivity analysis of parameters affect borehole stability.

Variables	Rate of change		
	Variables	Collapse pressure	Breakdown pressure
Thermal expansion coefficient	50%	0.38%	1.24%
	−50%	−0.38%	−1.23%
Borehole temperature	100%	0.76%	2.47%
	−200%	−1.52%	−4.94%
Poisson's ratio	36.4%	0.09%	−1.67%
	54.5%	−0.10%	2.61%
Pore pressure	10%	3.17%	0.00%
	−10%	−3.17%	0.00%
Overburden stress	10%	11.30%	−5.39%
	−10%	−11.30%	5.39%
Maximum horizontal stress	10%	−3.39%	4.85%
	−10%	3.39%	−12.65%
Minimum horizontal stress	7.2%	0.00%	6.00%
	−15.6%	0.00%	−15.92%
Well inclination	−50%	−9.61%	11.20%
	−100%	−19.21%	16.41%

When using the water-based mud, the temperature along the horizontal section of the wellbore is below the static formation temperature, which makes the critical mud weight window narrower and move downward, as shown in Fig. 12.

Because of the sufficient heat exchange in the long horizontal section, the temperature variation magnitude in horizontal well is smaller than that in vertical by using either mud system, and the bottom hole temperature in horizontal well is more close to the static formation temperature. However, the effect of thermal stress on critical mud weight window in horizontal is more sensitive, therefore, the thermal effect on wellbore stability for different situations should be calculated with specific well geometry, material properties and downhole environment.

4. Uncertainty analysis

Many parameters affect borehole stability. These parameters include three principal stresses, pore pressure, mud weight, well azimuth and inclination, borehole temperature. The problem of applying a borehole stability model is that none of these parameters can be accurately measured. Thus, in this section the uncertainty analysis provide a confidence level to each calculated safe mud weight range, parameters in Section 3.2 were used as a basis for the uncertainty analysis, and the results are shown in Table 3.

From Table 3, we can see that when $\sigma_V > \sigma_H > \sigma_h$, the parameters impacting on the safe mud weight to stabilize borehole are well inclination followed by three principal stresses, pore pressure, borehole temperature, thermal expansion coefficient and Poisson's ratio. The thermal expansion coefficient, Poisson's ratio and borehole temperature have an insignificant effect on collapse mud weight. Pore pressure have an insignificant effect on breakdown mud weight.

5. Conclusions

An integrated circulation temperature model for horizontal well drilling was established and field-tested. Horizontal well thermal performance is quite different from that for vertical wells, bottom hole circulating temperature for horizontal wells can sometimes exceed the formation temperature at the same depth.

Because of the sufficient heat exchange in long horizontal section, the temperature variation magnitude in horizontal well is smaller than that in vertical wells; however, the effect of thermal stress on critical mud weight window in horizontal well is more sensitive.

When the bottom hole temperature exceeds the static formation temperature by using oil-based mud, the critical mud weight window at toe of horizontal section is larger than that at heel of horizontal section. Using the water-based mud will narrow down the critical mud weight window. Oil-based mud is recommended to use to minimize the cooling effect for the enlarging critical mud weight window purpose.

Acknowledgment

The authors wish to acknowledge the People's Republic of China “973 Projection” (Grant No. 2010CB226706) and National Natural Science Foundation of China (Grant No. 51334003, 51274045, 51274221 and 51374223) for the financial support.

Nomenclature

BHA	bottom hole assembly
C_P	specific heat capacity, J/(kg°C)
E	Young's modulus, MPa
h	convective heat transfer coefficient, W/(m^2 °C)
MWD	measurement while drilling
P_p	pore pressure, Equivalent, g/cm^3
P_i	hydraulic pressure
S_a, S_p	heat source term in annular and drilling pipe, respectively, J/m^3
S_0	cohesion, MPa
t	time, s
T	temperature, °C
v	velocity vector, m/s
α_B	Biot's constant
α_T	thermal expansion coefficients, °C^{-1}
α	wellbore deviation angle, °
β	the angle between wellbore azimuth and horizontal, °
θ	angle of circumference, °
λ	thermal conductivity, W/(m°C)
ρ	density, g/cm^3
σ_{bd}	breakdown stress, MPa
σ_H	maximum horizontal stress, MPa
σ_h	minimum horizontal stress, MPa
σ_t	tensile strength, MPa
σ_v	overburden stress, MPa
σ_{xx},σ_{yy}, σ_{zz}	the stress field of surrounding rock in wellbore Cartesian coordinate system, MPa
σ_r, σ_θ, σ_z,$\tau_{r\theta}$	the radial stress, the tangential stress, and the shear stress of surrounding rock or casing, MPa
υ	Poisson's ratio
Φ	formation porosity, %
φ	friction angle, °

References

Aadnoy, B.S., Belayneh, M., 2008. A New Fracture Model That Includes Load History, Temperature, and Poisson's Effects. SPE 114829.
Edwardson, M.J., Girner, H.M., Parkinson, H.R., et al., 1962. Calculation of formation temperatures disturbances caused by mud circulation. J. Pet. Tech. 14 (4), 416–426.
Fjaer, E., Holt, R.M., Horsrud, P., Raaen, A.M., Risnes, R., 1992. Petroleum Related Rock Mechanics. Elsevier Science Publishers, Amsterdam.
Furui, K., Zhu, D., Hill, A.D., 2003. A rigorous formation damage skin factor and reservoir inflow model for a horizontal well. SPE Prod. Facil. 18 (3), 151–157.
Gonzalez, Manuel Eduardo, Bloys, James Benjamin, Lofton, John E., et al., 2004. Increasing Effective Fracture Gradients by Managing Wellbore Temperatures. IADC/SPE 87217.
Holmes, C.S., Swift, S.C., 1970. Calculation of circulating mud temperatures. J. Pet. Tech. 22 (6), 670–674.
Iyoho, A.W., Rask, J.H., Wieseneck, J.B., Grant, L.S., 2009. Comprehensive Drilling

Model Analyzes BHT Parameters. IADC/SPE 124142.
Kabir, C.S., Hasan, A.R., Kouba, G.E., Ameen, M., 1996. Determining circulating fluid temperature in drilling, workover, and well control operations. SPE Drill. Complet. 11 (2), 74–79.
Kumar, Aniket, Pratap Singh, Ajay, Samuel, Robello, 2012a. Analytical Model to Predict the Effect of Pipe Friction on Downhole Temperatures for Extended-reach Drilling (ERD). IADC/SPE 151254.
Kumar, Aniket, Pratap Singh, Ajay, Samuel, Robello, 2012b. Field Application of an Analytical Model for Estimating the Downhole Temperatures Due to Wellbore Friction. IADC/SPE 156307.
Li, Zhuoyi, Zhu, Ding, 2010. Predicting flow profile of horizontal well by downhole pressure and distributed-temperature data for waterdrive reservoir. SPE Prod. Oper. 25 (3), 296–304.
Marshall, D.W., Bentsen, R.G., 1982. A computer model to determine the temperature distributions in a wellbore. J. Cdn. Pet. Tech. 21 (1), 63–75.
Nguyen, D., Miska, S., Yu, M., Saasen, A., et al., 2010. Modeling Thermal Effects on Wellbore Stability. SPE 133428.
Nansheng, Qiu, Sehngbiao, Hu, Lijuan, He, 2004. Theory and Application of Sedimentary Basin Thermal System. Petroleum Industry Press (in Chinese).
Perkins, T.K., Gonzalez, J.A., 1984. Changes in Earth stresses around a wellbore caused by radially symmetrical pressure and temperature gradients. Soc. Pet. Eng. J. 24 (2), 129–140.
Ramey Jr., H.J., 1962. Wellbore heat transmission. J. Pet. Tech. 14 (4), 427–435.
Raymond, L.R., 1969. Temperature distribution in a circulating drilling fluid. J. Pet. Tech. 21 (3), 333–341.
Tang, Lin, Luo, Pinya, 1998. The Effect of the Thermal Stress on Wellbore Stability. SPE, 39505.
Tragesser, A.F., Crawford, P.B., Crawford, H.R., 1967. A method for calculating circulating temperatures. J. Pet. Tech. 19 (11), 1507–1512.
Trichel, Keith, Fabian, John, 2011. Understanding and Managing Bottom Hole Circulating Temperature Behavior in Horizontal HT Wells – a Case Study Based on Haynesville Horizontal Wells. SPE/IADC 140332.
Wooley, G.R., 1980. Computing downhole temperatures in circulation, injection, and production wells. J. Pet. Tech. 32 (9), 1509–1522.
Xu, Z.L., 1982. Elastic Mechanics. 2nd People's Education Press (in Chinese).
Yoshioka, K., Zhu, D., Hill, A.D., Dawkrajai, P., Lake, L.W., 2007. Prediction of temperature changes caused by water or gas entry into a horizontal well. SPE Prod. Oper. 22 (4), 425–433.
Yu, M., Chen, G., Chenevert, M.E., 2001. Chemical and Thermal Effects on Wellbore Stability of Shale Formations. SPE 71366.